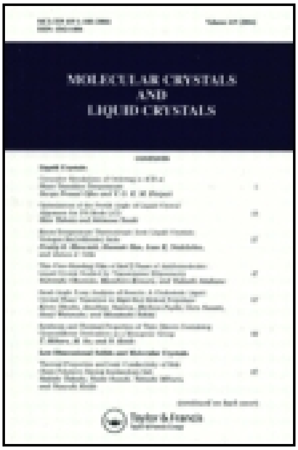

Molecular Crystals and Liquid Crystals
Publication details, including instructions for authors and subscription information:
http://www.tandfonline.com/loi/gmcl16

Calorimetric study of Nematic-Smectic-A_1 and Smectic-A_1-Smectic-A_2 transitions: T7, T8 and DB_6 + TBBA

C. Chiang [a] & C. W. Garland [a]
[a] Department of Chemistry and Center for Materials Science and Engineering, Massachusetts Institute of Technology, Cambridge, MA, 02139, USA
Version of record first published: 17 Oct 2011.

Mol. Cryst. Liq. Cryst., 1985, Vol. 122, pp. 25–34
0026-8941/85/1224–0025/$15.00/0

Calorimetric study of Nematic-Smectic-A_1 and Smectic-A_1-Smectic-A_2 transitions: T7, T8 and DB_6 + TBBA

C. CHIANG and C. W. GARLAND

Department of Chemistry and Center for Materials Science and Engineering, Massachusetts Institute of Technology, Cambridge, MA 02139 USA

(*Received July 30, 1984*)

High-resolution ac calorimetric studies have been carried out on heptyloxybenzoyloxy cyanostilbene (T7), octyloxybenzoyloxy cyanostilbene (T8), and a mixture of a hexylphenyl cyanobenzoyloxy benzoate (DB_6) and terephtal-bisbutyl aniline (TBBA). The heat capacity C_p exhibits a sharp, asymmetric peak near the second-order nematic (N)-smectic-A_1(SmA_1) transition in these systems, all of which possess a nematic phase that is stable over a very wide temperature range. For a DB_6 + 15% TBBA mixture, there is also a SmA_1 – SmA_2 transition at which C_p exhibits a distinct cusp. The critical exponent α is 0.05 (very close to a log singularity) for the N-SmA_1 transition and -0.14 for the SmA_1-SmA_2 transition. These values are in good agreement with critical x-ray studies but do not conform with current theoretical predictions.

INTRODUCTION

Extensive work at Bordeaux and Orsay has established the structures, phase diagrams, and some of the properties of a new class of polar liquid crystals containing aromatic cores with three phenyl rings.[1]

Typical examples of these compounds are

Tn alkoxybenzoyloxy cyanostilbene

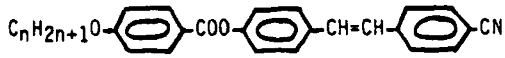

DB_n cyanobenzoyloxybenzoate of alkylphenyl

TBBA terephtal-bis-butyl aniline

Such compounds and their mixtures exhibit a rich variety of new smectic phases and complex reentrant behavior; see Figs. 1 and 2. In order to discuss the phase transitions shown in these figures, one must distinguish three types of smectic-A phase—SmA_d, SmA_1, and SmA_2. X-ray characterization by Levelut[2] has shown in all three cases that there is scattering corresponding to *two* wavevectors $q_z = q_1$ and q_2. These two wavevectors may or may not be commensurate. Figure 3 shows a schematic representation of the various types of smectic layers that can be formed by polar molecules of length L. The bilayer SmA_d phase involves the condensation of a quasi-Bragg peak at $q_1 = 2\pi/d$, corresponding to layers of thickness $d \simeq 1.7L$, with incommensurate fluctuations occurring at $q_2 = 2\pi/L$. The phase SmA_1 is a single-layer smectic with layers of thickness L (leading to a Bragg peak at q_2) and fluctuations at q_1 associated with cybotactic bilayer groups. The SmA_2 phase corresponds to a commensurate condensation of Bragg peaks at both wave vectors q_2 and $q_1 = q_2/2$. See Refs. 2 and 3 for further details.

A definitive analysis of the critical behavior near transitions involving these new smectic phases has not yet been made. However, there is a detailed mean-field treatment by Prost[4] and recent RNG extensions by Wang and Lubensky.[5] Briefly stated, current theory suggests that the N-SmA_1 transition should be in the XY universality class (with complications) and the SmA_1-SmA_2 transition should be in the Ising universality class.

The heat capacity data reported here together with correlated diffuse x-ray scattering data on DB_6 + TBBA[3] and T7[6] serve to

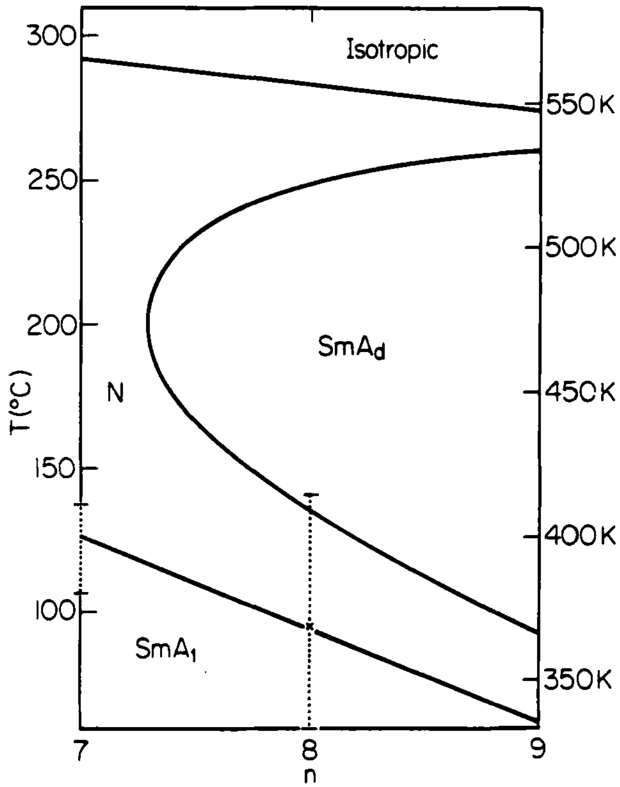

FIGURE 1 Phase diagram for the Tn system, indicating transitions for the pure compounds T7, T8 and T9 as well as binary mixtures of T7 + T8 and T8 + T9 (after Hardouin *et al.*[1]). The ranges of temperature studied calorimetrically are indicated by the dotted vertical lines.

characterize the critical exponents α (the heat capacity $C_p \sim t^{-\alpha}$, where t is the reduced temperature), ν (the correlation length $\xi \sim t^{-\nu}$), and γ (the order-parameter susceptibility $\sigma \sim t^{-\gamma}$). Such a combination of heat capacity and x-ray studies allows one to test the general concept of hyperscaling and to discuss better the universality class for $\mathrm{Sm}A_1$-$\mathrm{Sm}A_2$ and N-$\mathrm{Sm}A_1$ transitions.[7]

The high-resolution ac calorimeter used in this work has been described previously.[8] All the C_p values reported here correspond to the total heat capacity of a filled silver cell weighing $\sim 0.6g$, of which $\sim 0.1g$ is due to the liquid crystal sample. The heat capacity of the empty cell $C_p(e)$, which has an almost constant value of ~ 0.18 J K^{-1},

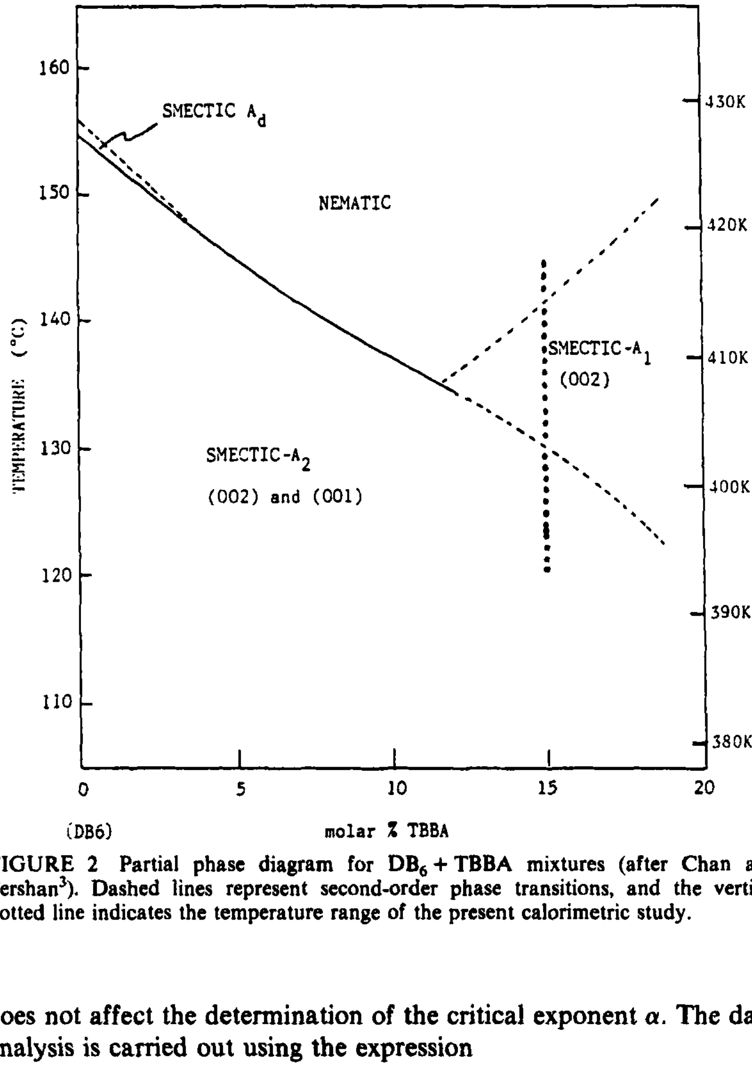

FIGURE 2 Partial phase diagram for $DB_6 + TBBA$ mixtures (after Chan and Pershan[3]). Dashed lines represent second-order phase transitions, and the vertical dotted line indicates the temperature range of the present calorimetric study.

does not affect the determination of the critical exponent α. The data analysis is carried out using the expression

$$C_p^{\pm} = A^{\pm}|t|^{-\alpha}(1 + D^{\pm}|t|^{.5}) + B + E(T - T_c), \qquad (1)$$

where T_c is the critical temperature for the phase transition, $t \equiv (T - T_c)/T_c$, and the superscript $\pm$ denotes $T > T_c$ or $T < T_c$. For the limiting case $\alpha \to 0$, one replaces Eq. (1) by

$$C_p^{\pm} = A \ln|t| + B^{\pm} + E(T - T_c). \qquad (2)$$

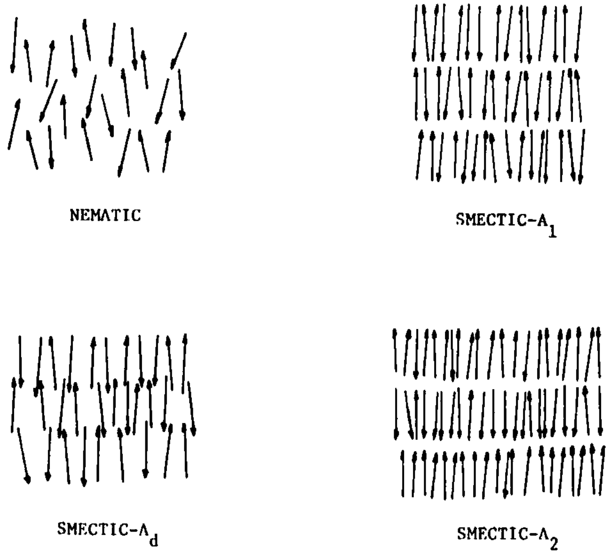

FIGURE 3 Schematic representation of the nematic and three smectic-A phases in polar long-core liquid crystals.

RESULTS FOR T7 AND T8

Figure 1 shows the range of temperatures covered by our measurements in T7 and T8. Note that T7 exhibits a very wide nematic range ($T_{NI} - T_{NA_1} = 166$ K). Even in T8, where reentrant behavior occurs, the reentrant nematic range ($T_{NA_d} - T_{NA_1} = 43.7$ K) is large compared to the nematic range in smectic liquid crystals having only two phenyl rings in the aromatic core.[7] Note that we shall not discuss here the very weak heat capacity peak at the second-order reentrant-nematic—smectic-A_d transition.

Details of the C_p variations near the N-SmA_1 transition in T7 and T8 are shown in Figs. 4 and 5. The smooth curve in each case represents the best least-squares fit to these data using Eqs. (1) with $\alpha = 0.05$. In the case of T8, the values of the least-squares parameters are quite stable to variations in the reduced temperature range used in the fitting procedure. In the case of T7, the parameters are fairly sensitive to range shrinking but the best fits seem to correspond well to those for T8. The minimum in χ^2 is rather broad, and we estimate that the uncertainty in α is ± 0.06. Thus these C_p data in T7 and T8 yield a N-SmA_1 critical exponent ($\alpha = 0.05 \pm 0.06$) that indicates a very weak power-law singularity. One cannot, however, rule out a

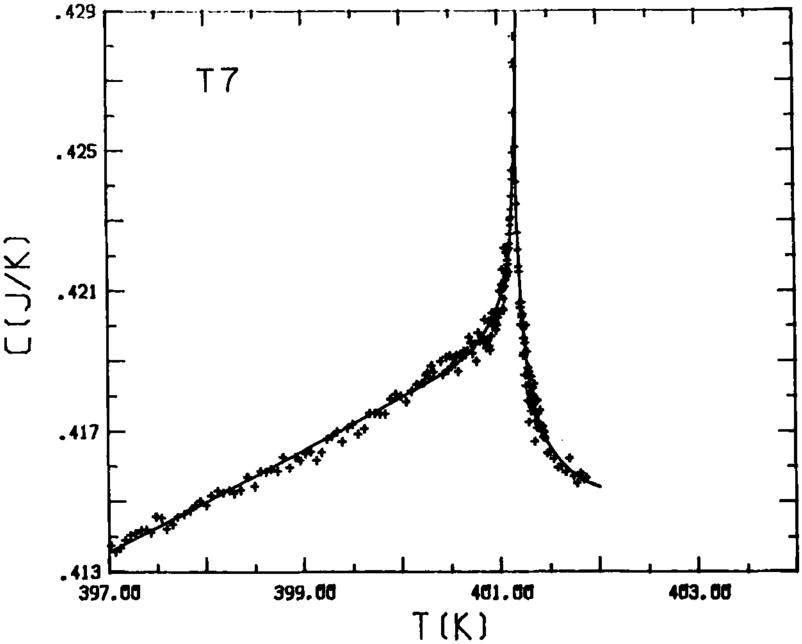

FIGURE 4 Heat capacity of T7 near the N-SmA_1 transition. The smooth curve represents the best fit with Eq. (1), and $\alpha = 0.05$.

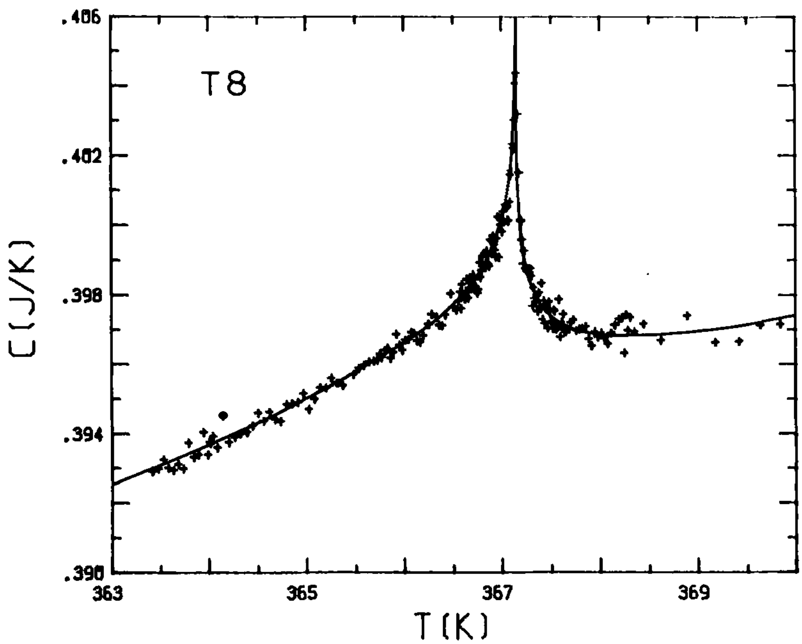

FIGURE 5 Heat capacity of T8 near the N-SmA_1 transition. The smooth curve represents the best fit with Eq. (1), and $\alpha = 0.05$.

sharp cusp such as that predicted for the XY model ($\alpha_{XY} \simeq -0.007$)[9] or a logarithmic divergence ($\alpha \rightarrow 0$). In terms of the exponent α, the critical behavior in T7 and T8 seems to be quite similar to that in $\bar{8}$S5 and 40.7, systems with nematic ranges of 20–25 K. However, the C_p(N-SmA_1) peaks in Figs. 4 and 5 are clearly more asymmetric than the C_p(N-SmA) peak for 40.7.[7] Furthermore, preliminary x-ray results on T7 indicate that $\gamma < \gamma_{XY}$ and $\nu_{\parallel} > \nu_{XY} > \nu_{\perp}$.[6] This implies that the Tn system exhibits anisotropic critical behavior at the N-SmA_1 transition which is not consistent with the XY model. Such a conclusion has been drawn previously for N-SmA_d and N-SmA_m transitions involving bilayer or monolayer smectics with short aromatic cores.[7] Further details of the analysis of both calorimetric and x-ray data for T7, T8 and their mixtures will be presented elsewhere.

RESULTS FOR DB_6 + TBBA

As shown in Fig. 2, only one DB_6 + TBBA mixture (corresponding to ~15 mole percent TBBA) has been studied calorimetrically at the

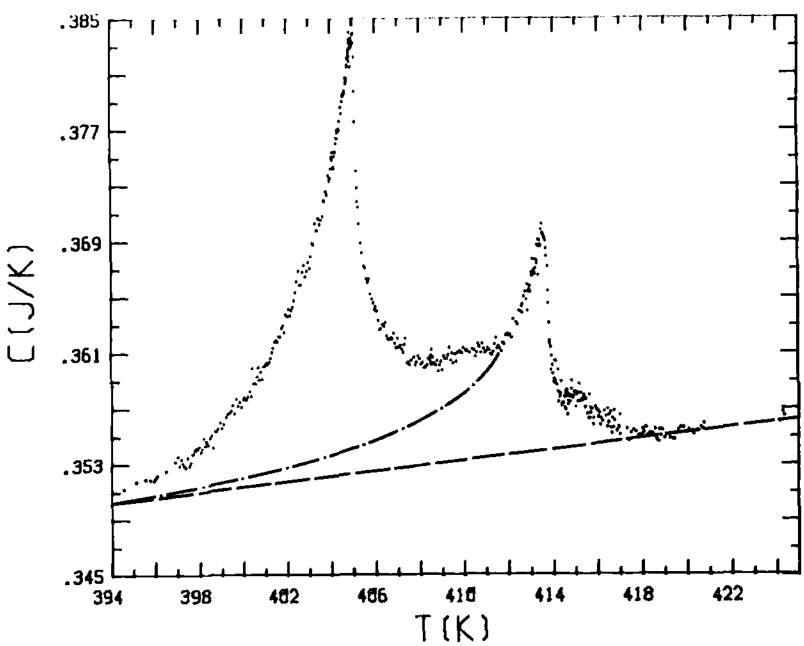

FIGURE 6 Heat capacity of DB6 + 15% TBBA. The linear C_p (background) variation is represented by the dashed line. The estimated low-temperature "tail" of the N-SmA_1 peak is shown by the dot-dash curve.

present time. The heat capacity variation for this sample over a wide temperature range is given in Fig. 6. These data allow us to estimate the linear C_p (background) that dominates the behavior far from any phase transitions. This C_p (background) variation is represented by the dashed line, and the dot-dash curve indicates the baseline under the SmA_1-SmA_2 peak due to the "tail" of the N-SmA_1 peak. (Compare this reconstruction of the N-SmA_1 excess heat capacity with Figs. 4 and 5.)

The detailed critical variation in C_p near the SmA_1-SmA_2 peak is shown in Fig. 7. The smooth curve represents the best least-squares fit using Eq. (1). The resulting value of the critical exponent α is $-0.14 \pm .06$, and the amplitude ratio A^-/A^+ is $0.55 \pm .1$. A full account of these data and their analysis will be reported elsewhere.[10]

An α value of -0.14 for the SmA_1-SmA_2 transition is consistent with recent x-ray results for the correlation lengths but differs greatly from the theoretically expected Ising value ($\alpha_I = +0.11$). The x-ray investigation of Chan, Sorensen and Pershan[3] yields $\gamma = 1.46 \pm 0.5$ and $\nu_{\parallel} = \nu_{\perp} = 0.74 \pm .03$ for the correlation exponents parallel and

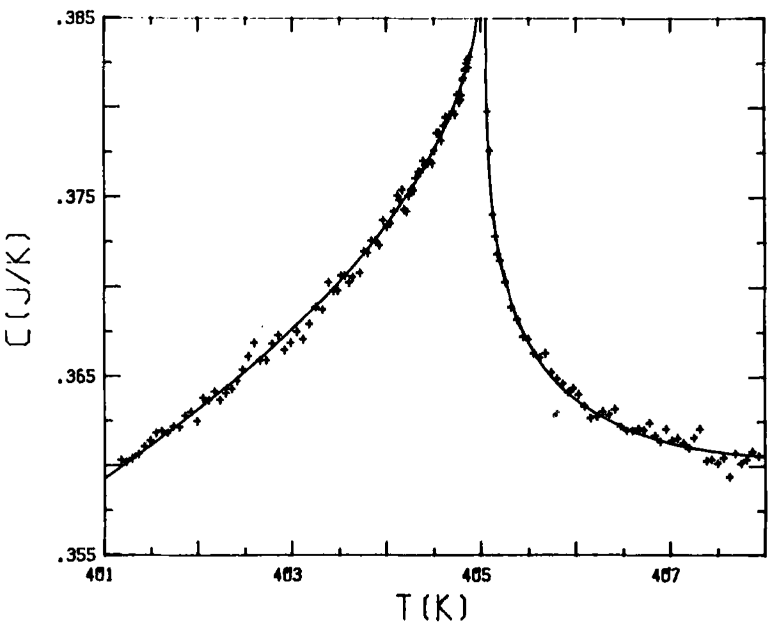

FIGURE 7 DB_6 + 15% TBBA heat capacity near the SmA_1-SmA_2 transition. The smooth curve represents the best fit with Eq. (1) and the resulting critical exponent is $\alpha = -0.14$.

perpendicular to the director. Thus the critical behavior of the correlation lengths is isotropic (unlike N-SmA transitions), and the hyperscaling relation $\alpha + 3\nu = 2$ is fairly well obeyed ($\alpha + 3\nu = 2.08 \pm 0.15$). This means that two completely independent experiments are consistent with each other, and both contradict the expected Ising behavior. A comparison between SmA_1-SmA_2 experimental behavior and theoretical Ising model behavior[9] is summarized below:

	α	A^-/A^+	ν	γ
Ising model	0.11	1.95	0.63	1.24
DB_6 + TBBA	$-0.14 \pm .06$	0.55	$0.74 \pm .03$	$1.46 \pm .05$

The C_p variation near the N-SmA_1 transition in DB_6 + 15% TBBA is shown in Fig. 8. The critical heat capacity peak associated with this transition is difficult to characterize since $T_c(N\text{-Sm}A_1)$ was observed to shift by -60 mK/hour for our sample. Figure 8 shows C_p vs $(T - T_c)$ for three runs in which data near T_c were obtained fairly

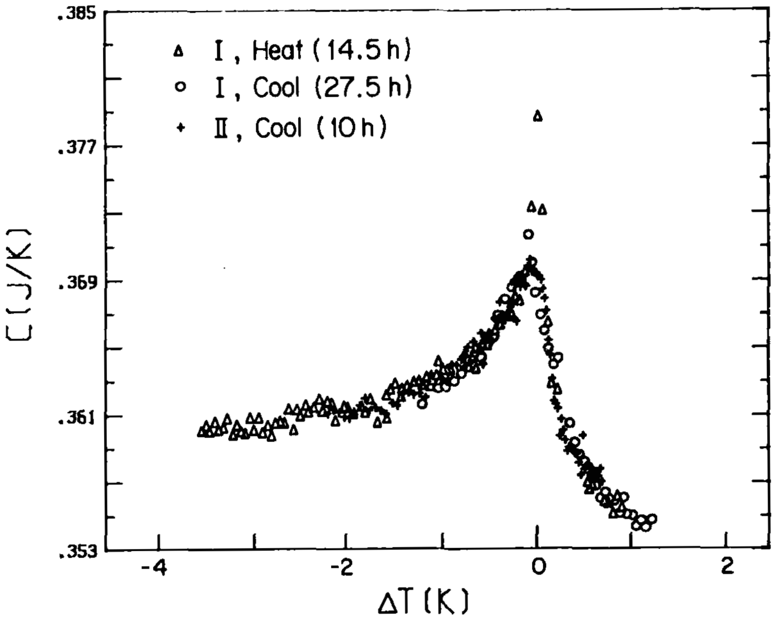

FIGURE 8 DB_6 + 15% TBBA heat capacity near the N-SmA_1 transition. The results for three runs are superimposed by plotting versus $T - T_c$. The length of time at high temperatures is $t_c - t_0$, where t_0 is the time the sample is placed in the high-temperature bath and t_c is the time when T_c is achieved.

soon after heating the sample from room temperature. These runs are in quite satisfying general agreement; and the N-SmA_1 critical heat-capacity peak is clearly similar to those in T7 and T8 but almost twice as large. However, no critical exponent analysis has been carried out on these data. Further experimental work on this and other compositions of DB_6 + TBBA mixtures is in progress, and the results will be reported elsewhere.

Acknowledgements

We wish to thank F. Hardouin and P. S. Pershan for helpful discussions. This work was supported by the National Science Foundation under contracts DMR-MRL 81-19295 and DMR 83-15637.

References

1. F. Hardouin, A. M. Levelut, M. F. Achard and G. Sigaud, *J. Chim. Physique* **80**, 53 (1983) and references cited therein.
2. A. M. Levelut, private communication; F. Hardouin, A. M. Levelut, J. J. Benattar, G. Sigaud, *Solid State Communications* **33**, 337 (1980); F. Hardouin, A. M. Levelut, G. Sigaud, *Journ. de Physique* **42**, 107 (1981).
3. K. K. Chan, L. B. Sorensen and P. S. Pershan, *Mol. Cryst. Liq. Cryst.*, to be published in this issue, and private communication.
4. J. Prost, J. Physique **40**, 581 (1979); J. Prost, *Springer Series in Chemical Physics* 11, *Liquid Crystals of One- and Two-Dimensional Order* (Springer Verlag, Berlin, 1980), p. 125.
5. J. Wang and T. C. Lubensky, *Phys. Rev.* **A29**, 2210 (1984).
6. B. M. Ocko and K. Evans-Lutterodt, private communication.
7. C. W. Garland, M. Meichle, B. M. Ocko, A. R. Kortan, C. R. Safinya, L. J. Yu, J. D. Litster, and R. J. Birgeneau, *Phys. Rev.* **A27**, 3234 (1983).
8. M. Meichle and C. W. Garland, *Phys. Rev.* **A27**, 2624 (1983); G. Sanchez, M. Meichle and C. W. Garland, *Phys. Rev.* **A28**, 1647 (1983).
9. J. C. LeGuillon and J. Zinn-Justin, *Phys. Rev. Lett.* **39**, 95 (1977); *Phys. Rev.* **B21**, 3976 (1980).
10. C. W. Garland, C. Chien and F. Hardouin, *Phys. Rev.* to be published.